Integrating Multiple Datasets in Google Earth Engine for Advanced Hydrological Modeling Using the Soil Conservation Service Curve Number Method

Mansoor Adil, Muhammad Azmat, Mudassir Sohail

Institute of Geographical Information System, School of Civil and Environmental Engineering, (NUST, Islamabad) Email: madil.ms21igis@student.nust.edu.pk, azmat@igis.nust.edu.pk, msohail.ms21igis@student.nust.edu.pk

*Corresponding Author: Mansoor Adil (madil.ms21igis@student.nust.edu.pk)

This research investigates the feasibility of using cloud computing and open-data sources for hydrological modelling. It uses Google Earth Engine (GEE) and the Soil Conservation Service Curve Number (SCS CN) approach to estimate runoff. The SCS CN approach is frequently used in the simulation of rainfall-runoff processes, and it is especially useful in estimating water intake into rivers, lakes, and streams. Google Earth Engine offers a variety of functionalities, algorithms for rapid data manipulation and visualization, and access to large global remote sensing and geographic information system (GIS) datasets. This study describes the development of an algorithm that uses Google Earth Engine (GEE) to observe precipitation data and produce antecedent moisture condition (AMC) maps. The algorithm uses the Soil Conservation Service Curve Number (SCS CN) method, which combines MODIS land use/land cover (LULC) data with USDA soil texture data to classify hydrological soil groups. The runoff is estimated using three datasets: CHIRPS, GPM, and TRMM. A detailed analysis of the relationship between rainfall and runoff in the Mangla watershed from 2005 to 2015 is performed. The study not only quantifies the runoff estimated by each rainfall dataset, but it also performs a comparison analysis of the datasets to ensure the accuracy and reliability of hydrological modelling. The rainfall-runoff analysis over a time period ten years (2005-2015) reveals large fluctuations in average rainfall and runoff levels, as well as evident seasonal tendencies. The highest average precipitation (1412.194 mm) was recorded in 2015 resulting in an average runoff of 215.021 mm. In contrast, the minimum average precipitation of 672.808 mm was recorded in 2009, resulting in an average runoff of 78.476 mm. The accuracy and validity of the modeled runoff observations are demonstrated through validation using observed meteorological data collected from Pakistan Meteorological Department (PMD), Water and Power Development Authority (WAPDA), and Climate Forecast System Reanalysis (CFSR). In the years 2008, 2009, and 2010, CHIRPS consistently proves better accuracies in comparison to GPM and TRMM, with accuracies of 90%, 79%, and 86% respectively. Furthermore, the sensitivity analysis conducted on the parameters of the SCS CN model reveals the impact of initial abstraction and Curve Number values on the estimation of runoff. In conclusion, this research work offers significant contributions to the understanding of hydrological processes in regions primarily influenced by monsoons and presents useful suggestions for the implementation of sustainable practices in water resource management.

Keywords: SCS CN Method, Hydrological Modeling, Runoff Estimation, CHIRPS, GPM, TRMM, Google Earth Engine, Cloud Computing.

Introduction:

Water resources are constrained and vital to human socioeconomic growth as well as to all other living creatures. The excessive use of water stresses the world's water supplies because of population growth and development activities. The rate of rise in water extraction worldwide over the past century has been six times higher than the rate of population growth. Physical water scarcity is imminent for 500 million people, accounting for one fifth of the global population. According to estimates, 65% of the world's aquatic ecosystems and river outflow are under danger of degrading [1]. The majority of the water needed for agricultural and home use might come from surface runoff. Nonetheless, there have been notable worldwide shifts in surface runoff [2]. The two main factors thought to be responsible for variations in surface runoff are anthropogenic activity and climate change [3][4]. Anthropogenic activities encompass any human-caused environmental disturbances, such as urbanization, deforestation, altered land use, and water usage for industrial and agricultural purposes [5].

One of the most significant hydrologic variables utilized in numerous applications linked to water resources is runoff. Its frequency and amount are determined by the strength, duration, and distribution of the rainfall event. Planning and managing water resources at the watershed level requires a detailed evaluation of a waters [5] hed's hydrologic response. Accurate surface runoff estimation is becoming more and more important in the hydrologic sciences because of its role in managing water resources. Quantification of surface and subsurface runoff is used by hydrologists for many different reasons. Hydrologic modelling, basin water monitoring, groundwater recharging, flood risk assessment, and water infrastructure design are a few of the uses for this measurement. Runoff data collecting from gauging stations is a difficult job that frequently requires costly installation and upkeep. Accessible runoff data that is global, continuous, and most importantly trustworthy is becoming increasingly and more significant.

The Natural Resources Conservation Services Curve Number (NRCS-CN) approach and its variants have been widely used in estimating runoff from ungauged watersheds. Compared to previous empirical and lumped parameter models, they have proven to be a faster and more accurate estimator of surface runoff [6]. The interplay of precipitation with the topography, land use, and physical characteristics of the soil of the land surface controls the hydrologic responses of the watershed that result in the formation of surface runoff. Because Geographic Information Systems (GIS) store and analyze the causal factors that lead to runoff generation, they are therefore preferable over traditional methodologies for accurately quantifying surface runoff. When the data required for CN-based runoff estimation approaches is saved, processed, and shown using a Geographic Information System (GIS), the estimation process becomes more interactive, efficient, and less labor-intensive.

The Natural Resources Conservation Service Curve Number approach (NRCS-CN), previously known as the Soil Conservation Service-Curve Number (SCS-CN) method, is a popular model for calculating rainfall runoff [7]. Since its inception by the USDA SCS in 1954, the technique has risen in popularity because to its simplicity, credibility, dependability, and capacity to respond to a wide range of parameters including soil type, land use, surface condition, and antecedent moisture condition. The NRCS approach was first developed in the United States to estimate runoff from storm rainfall events in agricultural watersheds. However, because of its convenience, water resource professionals have used it in a range of scenarios and land uses. The NRCS-CN approach has been successfully used to urban hydrology, rainwater harvesting, subsurface flow estimation, evapotranspiration (ET) calculation, and rainfall-runoff modelling. The NRCS-CN method's widespread use proves its utility in hydrologic applications [8]. Numerous methods for predicting global surface runoff need a significant amount of computer time. Satellite data, acquired in near real time, can provide reliable estimates of surface runoff at a spatial resolution relevant to hydrology. In this sense, this study provides a valid method for employing the NRCS-CN approach to estimate surface runoff in near-real time at

the pixel, watershed, regional, and global levels. The development of a nearly real-time terrestrial time-series runoff, particularly in ungauged watersheds, is critical for improving surface runoff and flood event estimates. Runoff estimations are used for flood predictions, hydrological engineering, agricultural planning, and water resource monitoring.

A global dataset for curve numbers at 250 m resolution, known as GCN250, was just released and made available to the public. GCN250 was validated using runoff from the Global Land Data Assimilation System (GLDAS), not gauge runoff data [9]. Using Google Earth Engine (GEE), the primary planetary-scale geospatial analytic tool, the dataset can be improved by altering the curve number based on its slope and then cross-referencing it with runoff data and remotely sensed real-time precipitation estimations. Using the GCN250 dataset, which considers wet, average, and dry antecedent runoff conditions, such an application will generate a global runoff generator building [9].

The Darewadi watershed is the topic of [10], which uses the Soil Conservation Service's (SCS) runoff curve number (CN) method for runoff estimation. The study focuses particularly on the integration of remote sensing (RS) and geographic information system (GIS) technologies. The Indian Meteorological Department's daily rainfall data was used during a 20-year period. The study demonstrates how the SCS-CN model can be used to calculate the depth of surface runoff when detailed hydrological data is not available. The study emphasizes the reliability and effectiveness of GIS and remote sensing in rapidly acquiring, processing, and understanding data for watershed planning. The SCS-CN model, which has been tailored to Indian settings, takes into account variables such as soil permeability, land use, and historical soil water conditions. The approach examines land use, soil type, and drainage basin boundaries. GIS makes it easy to compute curve numbers for runoff estimation. The study finds a considerable increase in maximum recharge capacity after 5 days of preceding rainfall and suggests that GIS is an essential tool for the tedious manual calculation of curve numbers for large regions. It calculates average curve numbers for pre- and post-treatment in the Darewadi watershed.

In [11] research work, the modified Soil Conservation System (SCS) Curve Number (CN) approach is utilized to investigate the estimation of rainfall and runoff, both of which are key components in hydrological research. The study uses GIS and remote sensing technology to estimate runoff efficiently in the Khuldabad taluka of Aurangabad District, India. The SCS-CN technique evaluates runoff potential by considering variables such as slope, vegetation cover, and watershed area. The researchers employed satellite data, GIS, and visual interpretation techniques to create digital databases and thematic maps for the study area. The SCS-CN method was used to estimate runoff on a daily, monthly, and annual scale. The findings revealed varying patterns of rainfall during a ten-years period (2003-2012). The computed runoff displayed a changing pattern, with 2010 having the greatest annual runoff. The correlation coefficients for daily, monthly, and annual runoff all indicate strong relationships, with annual runoff having the best fit. The study emphasizes the usefulness of SCS-CN methodology and GIS technology in water resource management in the area, as well as providing detailed information about the watershed's hydrological dynamics.

[12] provide a modified version of the Soil Conservation Service Curve Number (SCS-CN) approach, which is a prominent model for estimating surface runoff. The split of antecedent moisture condition (AMC) into three stages causes challenges for the existing SCS-CN approach in terms of unexpected increases in anticipated runoff. Previous attempts to solve these problems, such as the technique provided by [13] have improved but not eliminated structural inconsistencies. The proposed modification improves the Soil Moisture Accounting (SMA) procedure by including storm duration for more accurate estimates and resolving structural discrepancies. Furthermore, a physical formulation with wide application in simulating soil moisture dynamics is described and validated using soil water data from an experimental plot.

This enables the estimation of antecedent soil moisture (V0). In an evaluation utilizing a dataset from two experimental watersheds, the revised strategy outperformed the original SCS-CN and [13] methods with an efficiency of 88% in both the calibration and validation situations. The report emphasis the enhanced surface runoff forecast accuracy of the proposed system and urges for additional research to assess its robustness and potential simplifications.
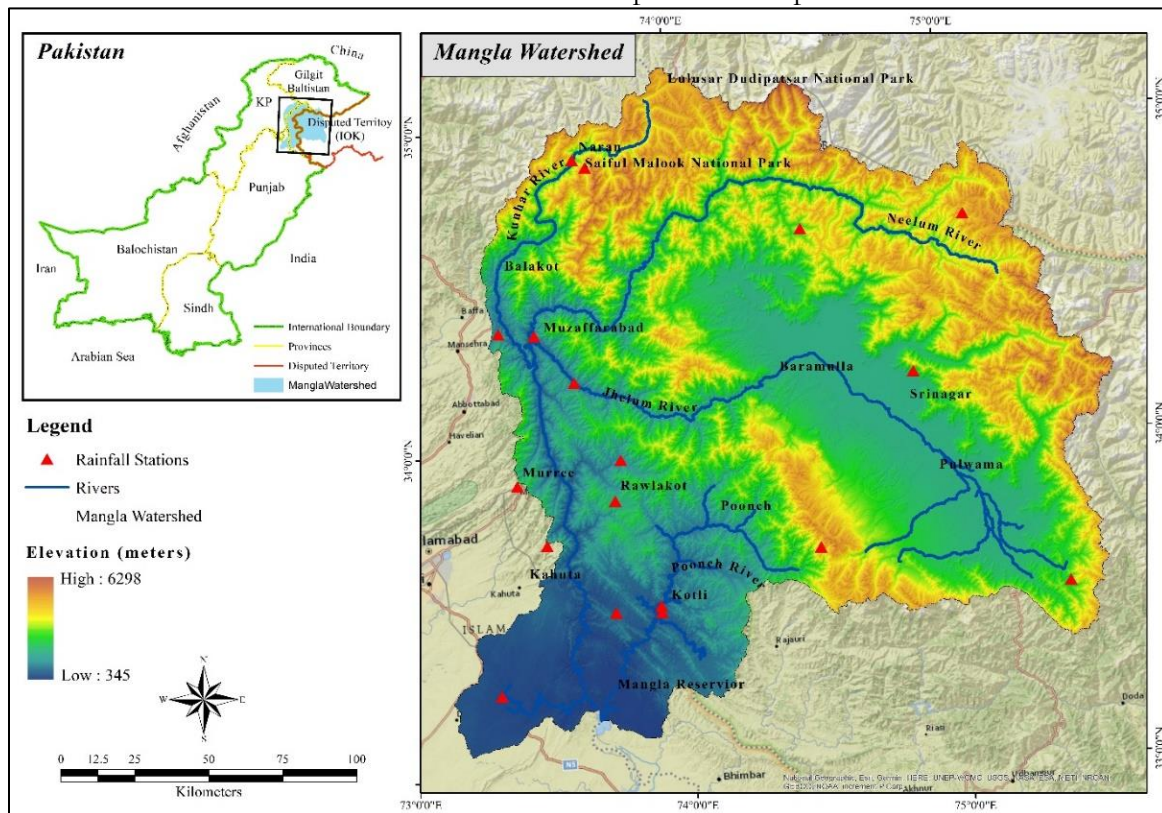

Figure 1: Study Area - Mangla Watershed

Study Area:

The Mangla Basin in northeast Pakistan has a watershed area of 33,419 km² and consists of seven major sub-basins: Neelum, Poonch, Kunhar, Upper Jhelum, Kanshi, Lower Jhelum, and Kahan. Every sub-basin has unique characteristics because of differences in catchment size and terrain slope [14]. The basin's hydrological dynamics are influenced by its topography, which ranges from gently undulating lands to abrupt cliffs and hilly terrain. The Mangla reservoir receives its water input in a predictable seasonal rhythm, with the majority of the inflow occurring between March and August and peaking in May. On the other side, the reservoir receives relatively little flow from October to February, typically less than 400 m3/s until snowmelt begins in March, triggering a rise in water flow that peaks in mid-May. The basin's climate varies greatly, owing primarily to elevation differences [15]. As elevation increases from south to north, the climate shifts from subtropical to temperate. At higher elevations, temperatures drop below freezing. The distribution of precipitation patterns is bi-modular, with peaks in March due to snowfall and in July due to monsoon rains. The Kunhar sub-basin's steep northern portions receive the highest precipitation, significantly influencing the basin's hydrological regime [16]. Temperatures vary greatly throughout the basin, with summer temperatures reaching up to 50 °C in the south and winter temperatures plunging below freezing in the north [17]. The Mangla Basin's unique terrain is the result of intricate interplay between hydrological processes, climate variations, and topography factors. This emphasizes the basin's importance in efforts to manage water supplies and improve regional environmental sustainability [18].

Methodology:

To create a script for the SCS CN model using cloud data and the GEE server, various data availability sources were investigated. A flowchart and script were used to finalize the methodology, which included data on land cover, rainfall (CHIRPS, GPM, and TRMM), and soil texture (FAO). The image below depicts the entire process of this study.
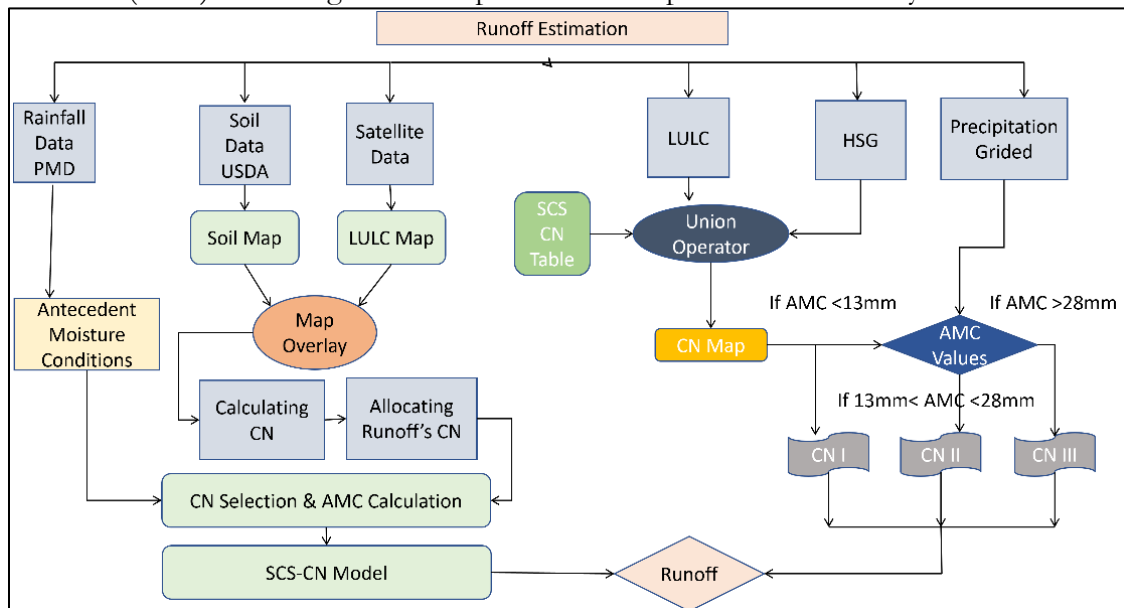

Figure 2: Methodology Flow Chart

Development of SCS CN Model:

As specified in the Soil Conservation Service (SCS) by the National Engineering Handbook (NEH-4) Section of Hydrology [19][20] the SCS–CN (1985) model was established in 1954 by the USDA SCS [21]. SCS-CN technique is predicated on the water balance computation [22]. The CN method, a lumped rainfall–runoff model that is event-based, is derived from the following water budget equation.

$$Q = \frac{(P-Ia)^2}{(P-Ia)+S} \qquad P > Ia \text{ Equation i}$$

where:

Q = runoff depth, in mm
P = rainfall depth, in mm
Ia = initial abstraction, in mm
S = surface retention maximum potential, in mm

The primary components of initial abstraction are surface depression storage, infiltration during the initial stages of the storm, and interception. For small watersheds, where lag is negligible, it can be inferred from observed rainfall-runoff events as the precipitation that falls prior to the start of runoff. While surface conditions and land cover can be used to predict interceptions and surface depression storage, infiltration during the early stages of a storm is highly variable and depends on various elements such soil moisture, soil texture, and the intensity of the rainfall. It's difficult to establish a relationship for estimating I_a. As a result, it was believed that I_a depended on S, the maximum surface potential retention. The empirical relationship between I_a and S was expressed as;

$$Ia = 0.2S \text{ Equation ii}$$

The rainfall-runoff relationship is obtained by substituting initial abstraction Ia value into equation of discharge.

$$Q = \frac{(P-0.2S)2}{(P+0.8S)}\text{Equation iii}$$

Where P is the daily rainfall, Ia the initial abstraction, Q the direct surface run off, S the potential maximum surface retention. Using Ia = 0.2S, was used to determine the curve numbers in (NEH, [23].

Curve Number:

The Curve number as defined by the U.S Soil Conservation Service (1972) is given by;

$$CN = \frac{25400}{254+S} \quad \textbf{for S in millimeters (mm)} \quad \textbf{Equation iv}$$

$$CN = \frac{1000}{10+S} \quad \textbf{for S in inches (inch)} \quad \textbf{Equation v}$$

Where **S** the potential maximum surface retention and CN is a unitless run-off coefficient that depends on land use (LU), hydrological soil type and AMC [24].
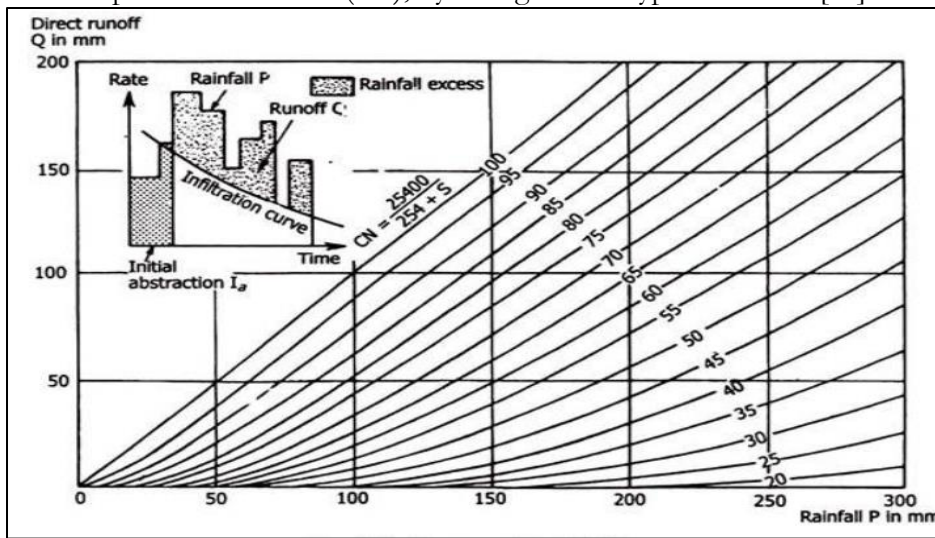

Figure 3: Curve Number Values for equation Q=(P-0.2S)2/(P+0.8S)

The amount and duration of rainfall, soil moisture content, land cover density, all contribute to the fluctuation in the CN. The Antecedent Moisture Condition (AMC) is a collective term for these sources of variability. Antecedent moisture is a catchment's relative wetness or dryness, which varies over time and has a big impact on run-off. Three classes can be distinguished within AMC.

- AMC I- Wet conditions with lowest runoff potential
- AMC II- Average Conditions with moderate runoff potential
- AMC III- Heavy rainfall with greatest runoff potential

Antecedent moisture conditions are determined using the previous five (5) days antecedent rainfall.

Table 1: AMC conditions using the 5 days antecedent rainfall.

Group	Soil Characteristics	Five-day antecedent rainfall in mm	
		Dormant Season	**Growing Season**
AMC I	Wet Conditions	>13	>36
AMC II	Moderate Conditions	Between 13 to 28	Between 36 to 53
AMC III	Heavy Rainfall	<28	<53

LULC and soil group conditions have been combined to generate CNs for AMC II. The following equations can be used to obtain CN for AMC I and AMC III equations [25][26].

$$CN\ I = \frac{4.2 \times CN\ II}{10-0.058 \times CN\ II} \text{ Equation (vi)} \qquad CN\ III = \frac{23 \times CN\ II}{10+0.13 \times CN\ II} \text{Equation(vii)}$$

According to antecedent soil moisture condition (AMC) and land use/cover (LU/LC), the SCS curve number determines a soil's capacity to permsit water infiltration [27]. According to the U.S. Soil Conservation Service (SCS), soils are categorized into four hydrologic soil groups, A, B, C, and D, based on the likely and eventual infiltration rates of runoff. To evaluate

the hydrological characteristics of the soil, soil texture data from the USDA Open Land Map were transformed into hydrological soil groups. Based on predetermined criteria, four hydrological groups (A, B, C, and D) were established from the soil texture classes, which indicate the relative amounts of sand, silt, and clay particles in the soil [28].

Table 2: The four USDA hydrologic soil groups (HSGs) are described as;

Hydrological Soil Groups	Description
HSG (A)	Sand & Sandy Loam
HSG (B)	Silty Loam & Loam
HSG (C)	Sandy Clay Loam
HSG (D)	Silt &Silty Clay Loam

Table 3: Datasets Used in this research work

S/N0	Data	Type	Dataset Availability
1	TRMM, CHIRPS and GPM	Rainfall data	1998-2020
2	Open Land Map Soil Texture Class (USDA System)	Soil data	1950-2018
3	MODIS Land Cover Type Yearly Global 500m	LULC	2001-2021
4	Digital Elevation Model (SRTM)	DEM	2000
5	Station rainfall data of PMD and WAPDA	Rainfall data	1960-2020

Table 4: Mangla Watershed LuLc Area in Sq-Km

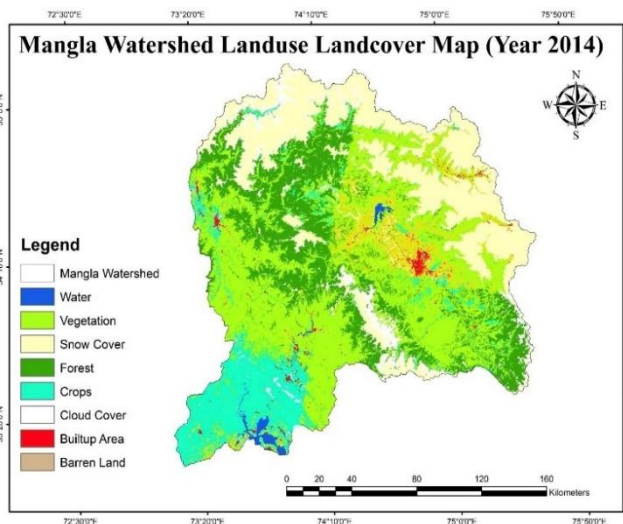| LuLc Type	Area_SqKm
Water	340
Forest	9851
Crops/Agriculture	3311
Built-up Area	4515
Bare Land	1126
Snow Covered	1610
Vegetation	12666
Total	**33419**

Figure 4: Mangla Watershed Land Use Land Cover Map

A comprehensive assessment was done to classify land use and land cover (LULC) within the Mangla watershed. The results of the land use and land cover (LULC) study exhibited a wide array of land cover categories throughout the watershed. Notably, forests constitute a significant proportion, spanning 9,851 square kilometers, which corresponds to 29% of the total land area. The region's agricultural activities are reflected in the 3,311 square kilometers (10%) of crops and agricultural grounds. The urban and infrastructural development within the watershed is indicated by the built-up area, which covers 4,515 square kilometers (14%). In addition, there is 1,126 square kilometers (3%) of bare ground and 1,610 square kilometers (5%) of snow-covered regions. The primary attribute of the terrain is vegetation, including a total area of 12,666 square kilometers, which accounts for approximately 38% of the total land area.

Mangla Watershed Soil Texture Map:

Within the study area, two distinct hydrological soil types have been identified, namely Group C (Sandy loam) and Group D (Clay loam). The predominant soil type identified across

the study area is Sandy loam soil. Sandy loam soil is characterized by an average soil texture, exhibiting a fairly uniform distribution of sand, silt, and clay particles. It is commonly observed in regions characterized by moderate to high levels of precipitation.
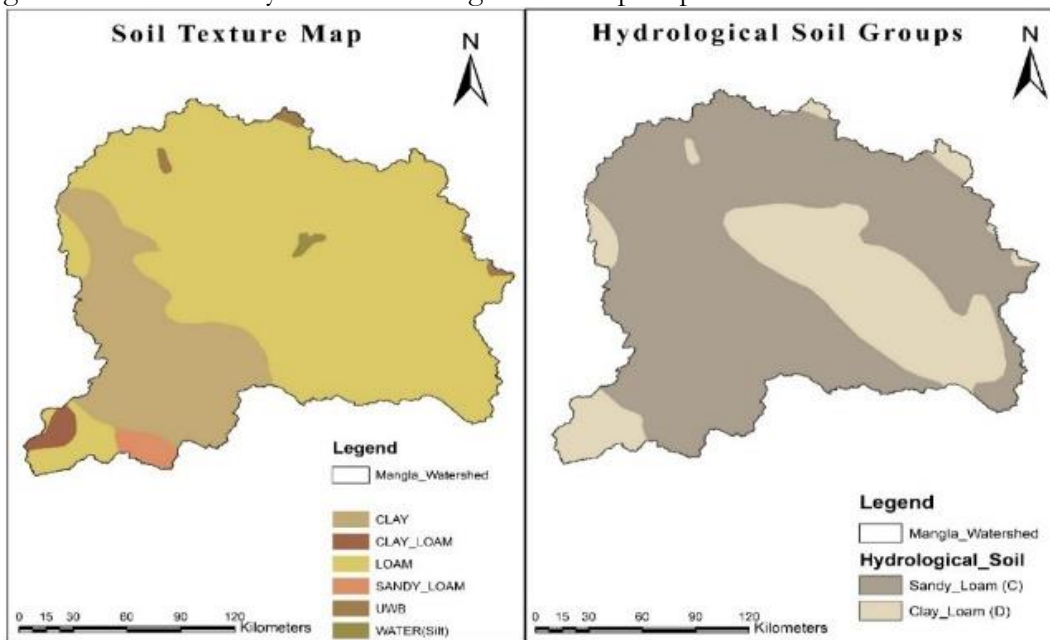

Figure 5: Mangla Watershed Soil Map

Soil data were characterized using soil texture data from the Open Land Map Soil Texture Class (USDA System) on Google Earth Engine [29]. Soil texture, or the relative proportions of sand, silt, and clay particles in the soil, has a substantial impact on soil fertility, water retention capacity, and overall soil quality.

Table 5: Hydrological Soil Group vs Runoff Potential

Hydrological Soil Group	Soil Type	Runoff Potential	Infiltration Rate mm/hr
HSG (A)	Sand & Sandy Loam	Low	Greater than 7.5
HSG (B)	Silty Loam & Loam	Medium	Between 3.8 to 7.5
HSG (C)	Sandy Clay Loam	Medium	Between 1.3 to 3.8
HSG (D)	Silt & Silty Clay Loam	High	Less than 1.3

Precipitation Datasets:

In this research we used three commonly utilized rainfall datasets to investigate precipitation patterns. These datasets include the Tropical Rainfall Measuring Mission (TRMM), the Global Precipitation Measurement (GPM), and the Climate Hazards Group Infrared Precipitation with Station Data (CHIRPS). CHIRPS combines a unique mix of in-situ station data and satellite photos with a resolution of 0.05° to provide highly precise gridded rainfall time series from 1981 to December 31, 2023 [30]. A groundbreaking global satellite effort known as the Global Precipitation Measurement (GPM) promises to change our understanding of global precipitation patterns IMERG, or Integrated Multi-satellite Retrievals for GPM, is the project's core component [31]. IMERG's fine-scale temporal resolution allows researchers to properly capture the intricacies of rainfall variability, with observations available every three hours. The GPM mission continues to lead global precipitation monitoring via constant validation and development, offering essential insights into the complexities of rainfall variability and its consequences for the environment and society [32]. The TRMM dataset provides researchers with precise insights into the global dynamics of tropical precipitation, with a temporal resolution of three hours and a spatial precision of 0.25 degrees. TRMM uses an advanced algorithm to gather satellite observations from many microwave devices in the constellation,

improving and interpolating precipitation estimates. Another element of the dataset is the RMS precipitation-error estimate, which increases the accuracy and dependability of rainfall data. It is critical to understand the complex connections between tropical rainfall patterns and wider climate dynamics [33].

Generating Curve Number Map:

Curve Number (CN) is a dimensionless parameter in hydrology that represents the runoff potential of a watershed or a specific geographical region. The Curve Number (CN) is an important component of several hydrological models, particularly the SCS-CN approach.

Table 6: CN Values for HSGs and Land Cover (USDA)

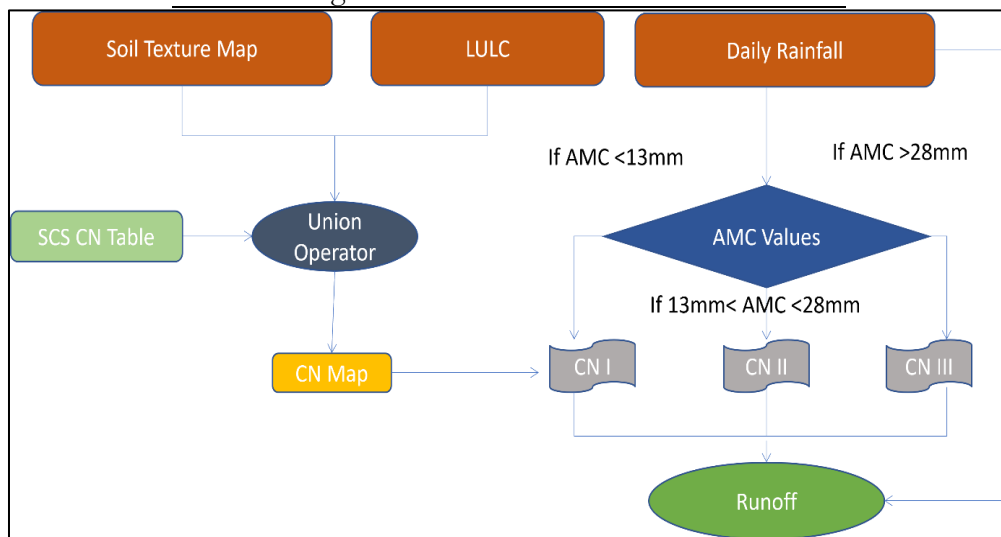| S. No	LuLc	A	B	C	D
1	Water	100	100	100	100
2	Trees	40	66	77	85
3	Terraced Crop	50	63	74	83
4	Build Up Area	81	88	91	93
5	Bare Land	68	79	86	89
6	Snow/Ice	98	98	98	98
7	Vegetation	63	77	88	88

Figure 6: Google Earth Engine Flow Chart [34].

SCS CN Model in GEE:

Google Earth Engine's vast collection of spatial data makes it simple to choose input data. Users can use a variety of filter methods to narrow down datasets from large image collections. Furthermore, GEE can handle dynamic data, but current models cannot. First, the image expression uses the ternary operator to arrange the soil texture map into four hydrologic soil groups (A, B, C, and D). Next, using the conditional statement, the curve number (CN II) map is created for each combination of the four soil groups and the 17 MODIS LULC data sets. The CN I and CN III equations are used to generate the CN I and CN III maps from CN II. The S image is AMC dependent and serves the same purpose as the CN image. As a result, during the final Q computation, the S values for the CN maps are formed. To minimize processing time, the script generates S images as a global variable for all CN conditions [34].

Create CN Map using JavaScript Expression:

CN values assigned to individual pixels were examined using the inspector tool in order to evaluate the dependability of the CN map. In order to do this, it was necessary to confirm if the given CN values matched the expected values for each land use land cover and soil hydrological group listed in the CN table provided by United States Department of Agriculture (USDA). For example, the expected CN value for water bodies should be between 98 and 100.

Using the inspection tool, we found that water bodies had a CN value of 100, confirming the accuracy of the CN values generated.

Table 7: Curve Number Expression using "IF" Statement

Soil Group A	Soil Group C
(a('soil') = 1) && (a('lulc') =1) 35	(c('soil') = 3) && (c('lulc') =1) 73
(a('soil') = 1) && (a('lulc') =2) 25	(c('soil') = 3) && (c('lulc') =2) 70
(a('soil') = 1) && (a ('lulc' =3) 45	(c('soil') = 3) && (c('lulc' =3) 77
(a('soil') = 1) && (a('lulc') =4) 39	(c('soil') = 3) && (c('lulc') =4) 74
(a('soil') = 1) && (a('lulc') =5) 45	(c('soil') = 3) && (c('lulc') =5) 77
(a('soil') = 1) && (a('lulc') =6) 49	(c('soil') = 3) && (c('lulc') =6) 79
(a('soil') = 1) && (a('lulc') =7) 68	(c('soil') = 3) && (c('lulc') =7) 86
(a('soil') = 1) && (a('lulc') =8) 36	(c('soil') = 3) && (c('lulc') =8) 73
(a('soil') = 1) && (a('lulc') =9) 45	(c('soil') = 3) && (c('lulc') =9) 77
(a('soil') = 1) && (a('lulc') =10) 30	(c('soil') = 3) && (c('lulc') =10) 71
(a('soil') = 1) && (a('lulc') =11) 95	(c('soil') = 3) && (c('lulc') =11) 96
(a('soil') = 1) && (a('lulc') =12) 66	(c('soil') = 3) && (c('lulc') =12) 85
(a('soil') = 1) && (a('lulc') =13) 72	(c('soil') = 3) && (c('lulc') =13) 87
(a('soil') = 1) && (a('lulc') =14) 63	(c('soil') = 3) && (c('lulc') =14) 83
(a('soil') = 1) && (a('lulc') =15) 100	(c('soil') = 3) && (c('lulc') =15) 100
(a('soil') = 1) && (a('lulc') =16) 73	(c('soil') = 3) && (c('lulc') =16) 90
(a('soil') = 1) && (a('lulc') =17) 100	(c('soil') = 3) && (c('lulc') =17) 100
Soil Group B	**Soil Group D**
(b('soil') = 2) && (b('lulc') =1) 51	(d('soil') = 4) && (d('lulc') =1) 78
(b('soil') = 2) && (b('lulc') =2) 55	(d('soil') = 4) && (d('lulc') =2) 77
(b('soil') = 2) && (b ('lulc' =3) 66	(d('soil') = 4) && (d ('lulc' =3) 82
(b('soil') = 2) && (b('lulc') =4) 61	(d('soil') = 4) && (d('lulc') =4) 81
(b('soil') = 2) && (b('lulc') =5) 66	(d('soil') = 4) && (d('lulc') =5) 82
(b('soil') = 2) && (b('lulc') =6) 69	(d('soil') = 4) && (d('lulc') =6) 90
(b('soil') = 2) && (b('lulc') =7) 79	(d('soil') = 4) && (d('lulc') =7) 89
(b('soil') = 2) && (b('lulc') =8) 60	(d('soil') = 4) && (d('lulc') =8) 79
(b('soil') = 2) && (b('lulc') =9) 65	(d('soil') = 4) && (d('lulc') =9) 83
(b('soil') = 2) && (b('lulc') =10) 58	(d('soil') = 4) && (d('lulc') =10) 78
(b('soil') = 2) && (b('lulc') =11) 95	(d('soil') = 4) && (d('lulc') =11) 95
(b('soil') = 2) && (b('lulc') =12) 78	(d('soil') = 4) && (d('lulc') =12) 89
(b('soil') = 2) && (b('lulc') =13) 81	(d('soil') = 4) && (d('lulc') =13) 89
(b('soil') = 2) && (b('lulc') =14) 75	(d('soil') = 4) && (d('lulc') =14) 87
(b('soil') = 2) && (b('lulc') =15) 100	(d('soil') = 4) && (d('lulc') =15) 100
(b('soil') = 2) && (b('lulc') =16) 84	(d('soil') = 4) && (d('lulc') =16) 92
(b('soil') = 2) && (b('lulc') =17) 100	(d('soil') = 4) && (d('lulc') =17) 100

Rainfall:

After generating the Curve Number (CN) map, three rainfall datasets were used to assess the hydrological modelling process. To improve the hydrological modelling approach, three rainfall datasets were combined with the Curve Number (CN) map. The Climate Hazards Group InfraRed Precipitation with Station Data (CHIRPS) daily dataset [35] was utilized first, followed by the Global Precipitation Measurement, GPM [32] and Tropical Rainfall Measuring Mission (TRMM) [36] datasets. Notably, CHIRPS data was available with a temporal resolution of 24 hours, whereas TRMM and GPM data were available every three hours. Mathematical computations were used to convert TRMM and GPM data to daily values for consistency in analysis.
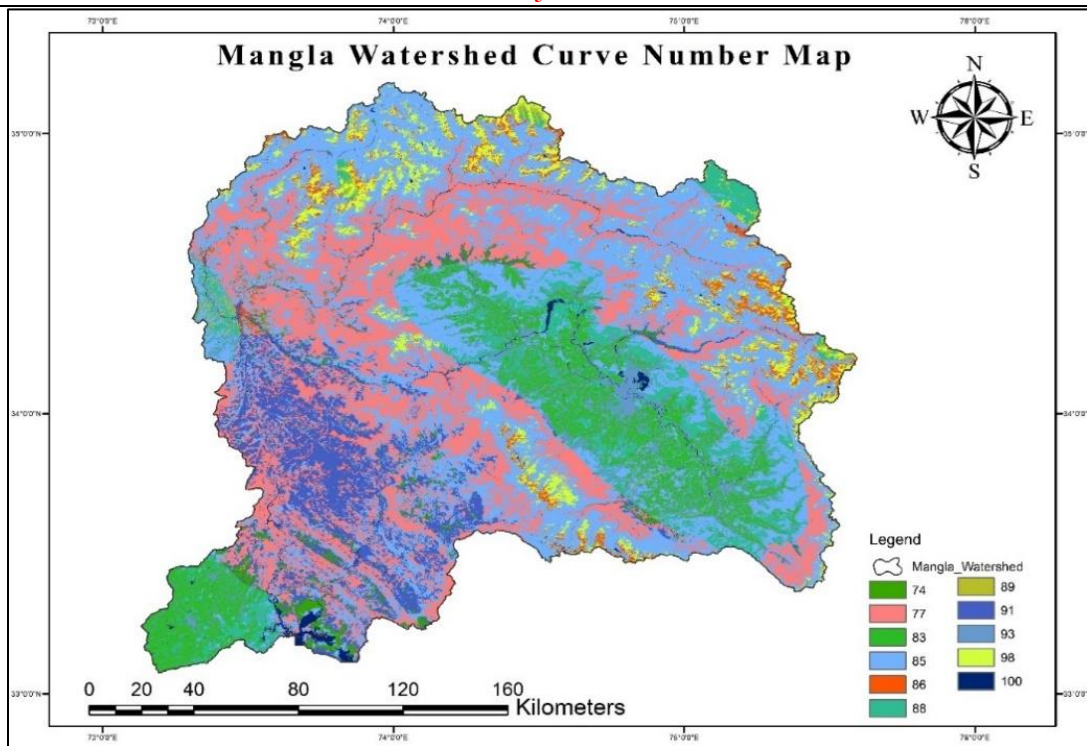
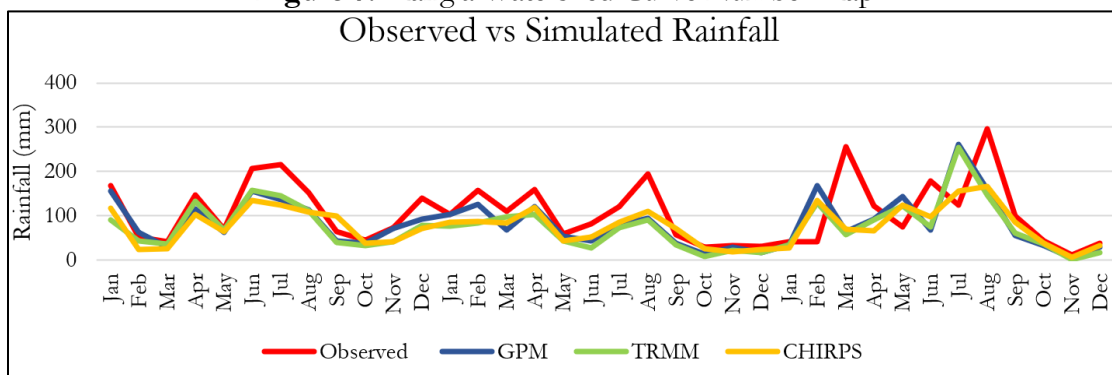**Figure 7:** Mangla Watershed Curve Number Map

Figure 8: Observed vs Simulated Rainfall Graph

Daily Antecedent Moisture Condition (AMC) images were generated based on rainfall data. First, the AMC value range for each pixel and day were examined. A Soil Moisture Condition (S) image was created based on each pixel's AMC value. In particular, the S-I image computed from CN I [40] was used to replace pixels with AMC less than 13 mm, while the S-III image computed from CN III was used to replace pixels with AMC greater than 28 mm. According to [40] pixels with AMC values of 13 to 28 mm retained their previous CN II values. Using this method, a single S image could be generated for each day, containing the appropriate soil moisture levels depending on the AMC values obtained throughout the study area. The S picture served as the foundation for further hydrological modelling and research. This provided insights into the constant interaction between runoff potential, soil moisture, and rainfall.

Table 8: Inventory of Climate stations

No.	Station Name	Latitude N	Longitude E	Elevation(m)	Data Source	Data Availability
1	Balakot	34.38	73.35	995	PMD	1962-2023
2	Ghari Dopatta	34.22	73.62	814	PMD	1961-2023
3	Kotli	33.52	73.90	614	PMD	1981-2023

| 4	Murree	33.90	73.39	2213	PMD	1961-2023
5	Muzaffarabad	34.37	73.48	686	PMD	1961-2023
6	Bagh	33.97	73.77	1067	WAPDA	1970-2009
7	Domel	33.71	73.49	702	WAPDA	1970-2009
8	Gujjar Khan	33.26	73.30	547	WAPDA	1970-2009
9	Naran	34.90	73.64	2362	WAPDA	1970-2009
10	Rawalakot	33.85	73.75	1676	WAPDA	1970-2009
11	Rehman Bridge	33.50	73.90	530	WAPDA	1970-2009
12	Saiful Maluk	34.88	73.69	3240	WAPDA	1970-2009
13	Sehr Kokata	33.50	73.73	915	WAPDA	1970-2009
14	Neelum	34.66	74.47	1035	CFSR	2000-2022
15	Baramulla	34.68	75.07	995	CFSR	2000-2022
16	Srinagar	34.20	74.86	1050	CFSR	2000-2022
17	Pulwama	33.67	74.49	1102	CFSR	2000-2022
18	Poonch	33.53	75.39	802	CFSR	2000-2022

*CFSR [37][38][39]
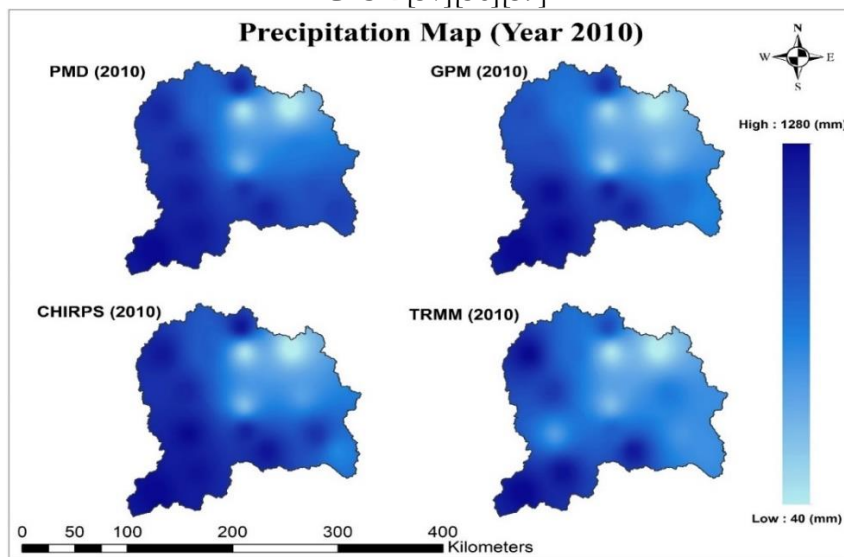
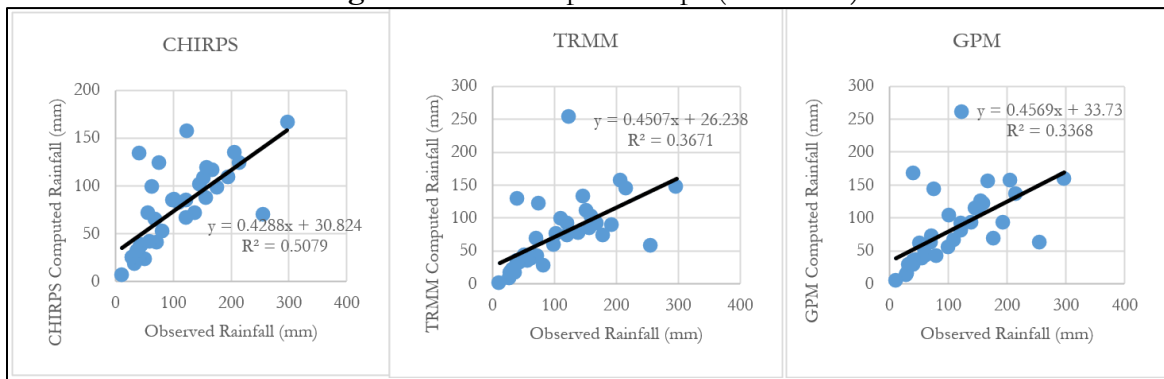**Figure 9:** Rainfall Spatial Maps (Year 2010)

Figure 10: CHIRPS, TRMM and GPM Computed vs Observed Rainfall

Results and Discussions:

The rainfall-runoff model was successfully developed on the Google Earth Engine (GEE) platform using the Soil Conservation Service Curve Number (SCS-CN) method. This model utilizes GEE's JavaScript API to incorporate essential data such as rainfall data, land use land cover (LULC) maps, and soil maps. To generate CN maps, the soil texture map was first classified as a soil hydrology group, and then integrated with LULC data. Antecedent Moisture

Conditions (AMC) were determined based on the total amount of precipitation received over the previous five days. The daily runoff was then calculated, considering the AMC conditions for each pixel.
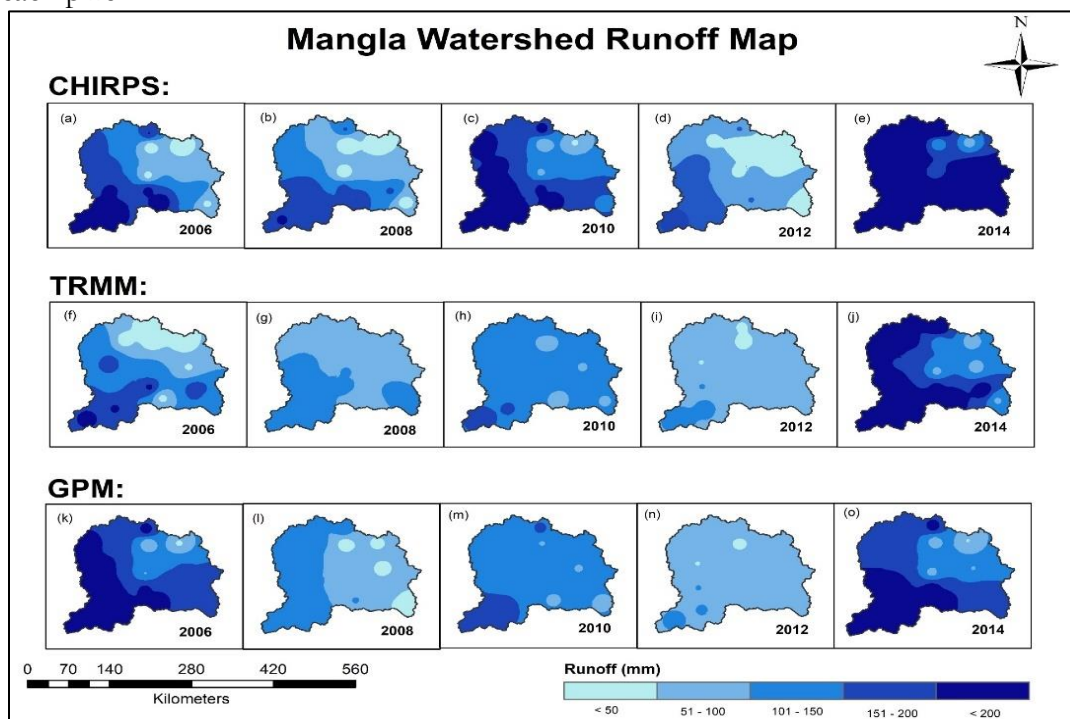

Figure 11: CHIRPS, TRMM and GPM Runoff Maps

The study area encompassed the Mangla watershed for ten years, from 2005 to 2015. It is important to emphasize that the study is based on the assumption that rainfall should always exceed runoff. Any occurrence in which runoff numbers exceed the amount of rainfall would indicate possible calculation error. The combined analysis of the CHIRPS, GPM, and TRMM datasets from 2005 to 2015 reveals important information about the patterns of summer monsoon rainfall in the Mangla watershed. Over a ten-year period, the datasets demonstrate unique seasonal fluctuations and general trends in rainfall patterns, illustrating the unpredictability of the summer monsoon with significant variances between years. Despite variations between the datasets, there is a consistent representation of the seasonal onset and withdrawal of the monsoon, with peak rainfall occurring during the monsoon months. Figure-10 shows yearly rainfall against each dataset with the corresponding runoff values generated. In 2005 highest rainfall 944.98mm was recorded for GPM resulting in a mean runoff of 83.829mm, followed by CHIRPS with a mean rainfall of 905.75mm, generating a runoff of 179.874mm. While the lowest rainfall for the year 2005 was recorded by TRMM with a mean value of 838.615mm resulting in a mean runoff of 127.20mm. Despite heavy rainfall only 8.8% of runoff was generated by GPM, this is because of the dry monsoon season where only 293mm rainfall was recorded which led to AMC I (lowest runoff potential). In 2006 a significant increase was observed in the rainfall values, for GPM it was 339mm taking the mean precipitation to 1283.321mm that resulted in a mean runoff of 242.89mm which increased the runoff value by 44%, for TRMM a mean rainfall of 1140.19mm was observed in the year 2006, resulting in a mean runoff of 210.77mm while for CHIRPS it was observed to be 1002.135mm generating a runoff of 241.74mm. Not much difference was observed in 2007,2008 and 2009 where a mean rainfall of 932.363, 948.24 and 800.15mm was recorded for CHIRPS resulting in a mean runoff of 210.80,202.97 and 119.12mm respectively. For GPM a rainfall of 867.92mm was observed in 2007, 1078.83mm in 2008 and 782.78mm in 2009. While the corresponding runoff values are 124mm, 140mm and 63.24mm respectively.

In 2010, a slight increase can be seen in the rainfall values which ultimately add off to the runoff values. For CHIRPS a mean runoff of 230.63mm was recorded, for TRMM it was observed to be 159.13mm and in case of GPM a mean runoff of 173.064mm was recorded. Next three years, 2011-2013 were relatively dry where a mean rainfall of 876.88mm was recorded for GPM, TRMM and CHIRPS, which resulted in a mean runoff of 132.2mm only. During the year 2014, which was dominated by heavy monsoon rainfalls high mean precipitation values were recorded. For CHIRPS it was observed to be 1244.064mm, for TRMM it was 1098.22mm while in case of GPM it was observed to be 1170.56mm resulting a mean runoff of 402.65,285.198 and 254.085mm respectively. In 2015 a rich pre-monsoon season was observed where a mean rainfall of 1228.064mm was observed for CHIRPS that resulted in a mean runoff of 283.82mm. on the other hand TRRM and GPM recorded a mean precipitation of 1175.79mm and 1412.19mm respectively, while their corresponding runoff vales were 287.36mm and 215.021mm. Overall an increasing trend was observed in the rainfall values from 2005 to 2015 for all the datasets. For rainfall values it was noticed that GPM led the charts while in case of runoff, CHIRPS was observed to be on the dominating side. TRMM seemed to be in transition for both rainfall and runoff.
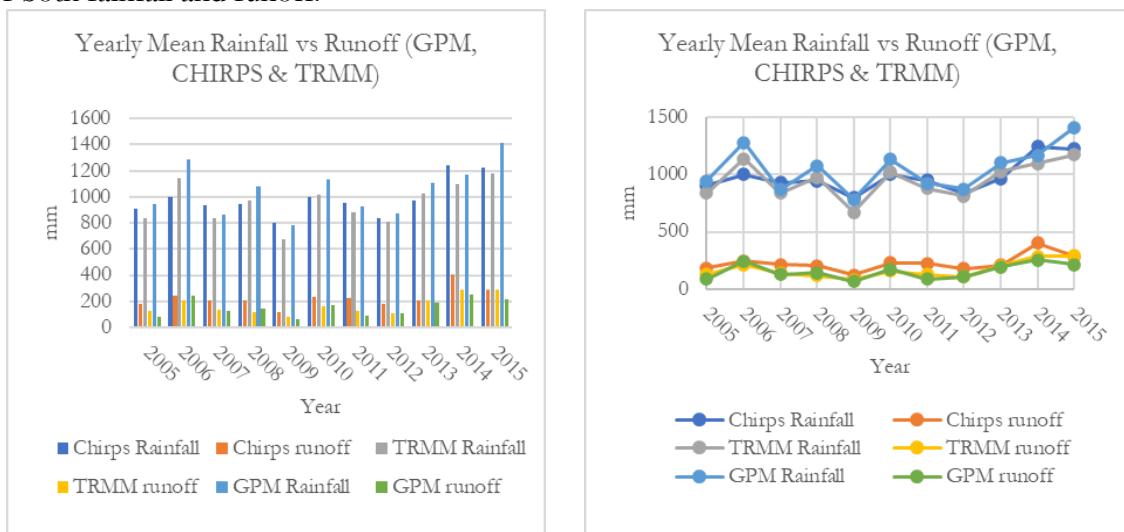

Figure 12: Yearly Rainfall vs Runoff (GPM, TRMM & CHIRPS)

Monsoon:

There are two sources of rainfall in the Indus River basin: the monsoon and the western disturbance [41]. Western disturbances begin in December and spersist until March, while the summer season runs from June to September. The Indian Monsoon, which is also known as the summer monsoon in South Asia, is a significant meteorological phenomenon that affects regional weather patterns and agricultural practices [42]. Heavy rains and strong winds are used to provide relief from the extreme heat leading up to the monsoon season, which lasts from June to September. In countries such as Pakistan [43] India, Bangladesh, and Nepal, the summer monsoon contributes significantly to yearly rainfall. This helps to keep agricultural activities running by giving water to crops and replenishing groundwater reserves [44]. We explored seasonal variation in precipitation properties over the Mangla watershed to compare the differences in seasonal variations in precipitation characteristics between TRMM, GPM, and CHIRPS, we chose three different years: 2006, 2010, and 2015. The target years were chosen based on the significant rainfall cycles that occurred across those years. Figure 11 shows the runoff values recorded against each rainfall dataset during the monsoon season, demonstrating the difference in runoff generation based on the recorded rainfall. For example, in June 2006, an average runoff of 20mm was recorded for CHIRPS rainfall, for GPM a runoff of 3.4mm, and for TRMM the recorded runoff was 3.5mm only. During the peak monsoon season in July

and August, CHIRPS records runoff values of 125mm in 2006, 112mm in 2010, and 73mm in 2015. GPM records runoff values of 146mm, 105mm, and 43mm for the respective years, while TRMM records 122mm, 80mm, and 42mm. Overall, CHIRPS exhibits the highest total runoff during the peak monsoon season, followed by GPM, with TRMM showing the lowest runoff values.
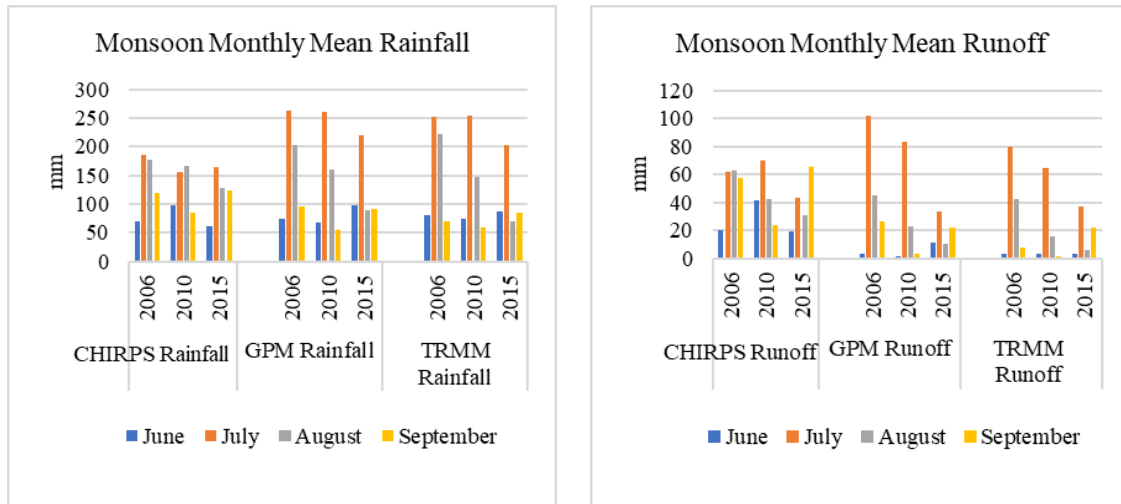

Figure 13: TRMM, GPM and CHIRPS Monsoon Rainfall and Runoff

Comparisons in year-to-year variations of seasonal mean monsoon rainfall for 3 different years (2006,2010 and 2015) of TRMM, GPM and CHIRPS was carried out. Yearly rainfall shows highest mean values for GPM 637mm in 2006 followed by TRMM with a mean rainfall of 623mm while the lowest yearly mean values of 552mm was observed in case of CHIRPS during the monsoon season year 2006.Interestengly the runoff calculated was highest 202mm for CHIRPS, 176mm recorded for GPM and lowest 133mm was observed in case of TRMM. Despite the lowest rainfall values for CHIRPS, highest runoff values were observed during 2006 monsoon season because of AMC III (highest runoff potential) conditions, which is a function of consistent rainfalls and high soil moisture content. Moving forward to monsoon 2010 where a mean rainfall of 505mm was recorded for CHIRPS resulting in a mean runoff of 176mm. In the case of GPM, during monsoon, a rainfall of 543mm was observed generating a runoff of 111mm in the year 2010. While in case of TRMM it was observed to be 535mm in 2010 monsoon season resulting in a mean runoff of 85mm only. In the year 2015 monsoon season the mean rainfall recorded for CHIRPS was 478mm resulting in a mean runoff of 158mm. For the same year (2015) GPM showed relatively higher rainfall values (499mm) during monsoon season, generating a mean runoff of 77mm. While TRMM in monsoon 2015 showed a mean precipitation of 443mm resulting a runoff of 67mm.

Results Validation:

For validation of results the observed daily meteorological data from year (1961-2022) were obtained from Pakistan Meteorological Department (PMD), Water and Power Development Authority (WAPDA) and Climate Forecast System Reanalysis (CFSR). The WAPDA stations are mainly for observing the flow discharge data, but they also observe certain climatic data such as precipitation and temperature data. An inventory of meteorological stations is displaced in Table-7. As Mangla Basin is a transboundary waterbody and we only have observed data of PMD and WAPDA which doesn't cover the entire basin that's why CFSR data were used along with PMD and WAPDA stations for the validation of results. CFSR data can be used in data scarce regions [38]. Out of 18 stations that were used for validation, data of five (5) stations were taken from CFSR database.

For the year 2008 the actual mean runoff calculated from the ground stations was 224.96mm while the observed mean runoff was 202.9mm for CHIRPS rainfall datasets, showing

a remarkable accuracy of 90%. While for GPM, a mean runoff of 140.5mm was observed with an accuracy of 62.5% only. The lowest accuracy of 52% was observed for TRMM rainfall datasets, where a mean runoff of 117mm was recorded during the year 2008. In 2009, the actual runoff recorded was 149.71mm while observed runoff for CHIRPS was 119.12mm (79% accuracy), 78.47mm (52% accuracy) for GPM and for TRMM a runoff of 63.24mm with an accuracy of 42% was observed. The mean runoff recorded was 267.37mm for the year 2010 while the observed mean runoff for CHIRPS, GPM and TRMM was, 230.63mm, 173.064mm and 159.19mm respectively with the highest accuracy of 86% by CHIRPS, 65% accuracy by GPM and about 60% accuracy was shown by TRMM.

Sensitivity Analysis:

As it is evident from the equation of SCS CN model that it requires only two input parameters one is initial abstraction value, and the second one is rainfall data.

$$Q = \frac{(P - Ia)^2}{(P - Ia) + S}$$

Where,

$$Ia = 0.2S$$

$$Q = \frac{(P - 0.2S)2}{(P + 0.8S)} \quad Equation(a)$$

$$CN = \frac{25400}{254 + S} \quad for\ S\ in\ millimeters\ (mm)$$

From equation (a) it is clear that basin recharge (S) depends on Curve Number value. So, we evaluated the model sensitivity for CN and S values. It can be clearly seen in the graph (Figure-12) that the estimated runoff was equal to zero when the CN values were less than 70 and then there is an increasing trend in the runoff values with increase in CN values. At CN=100 runoff values were equal to rainfall, as CN=100 represents waterbodies. On the other hand, in Figure-12 it can be observed that the runoff values decrease gradually as the initial abstraction values are increasing. Higher the Ia value lower will be the estimated runoff and vice versa. This comparative analysis confirmed that SCS CN model was much more sensitive to change in CN values and less sensitive to Ia values, and the same point is already endorsed [45].

Table 9: Results Validation against each Watershed

Objectid	Shape	LULC	Watershed	hydgrp	CN	Basin Recharge	Ia =0.2S
273523	Polygon	Built-up	WS-1	C	91	25.12088	5.024176
274025	Polygon	Vegetations	WS-1	C	85	44.82353	8.964706
274233	Polygon	Crops	WS-1	C	74	89.24324	17.84865
274980	Polygon	Barren Land	WS-1	C	86	41.34884	8.269768
275568	Polygon	Crops	WS-1	C	74	89.24324	17.84865
275615	Polygon	Trees	WS-1	C	77	75.87013	15.17403
381596	Polygon	Snow/Ice	WS-2	C	98	5.183673	1.036735
381683	Polygon	Trees	WS-2	C	77	75.87013	15.17403
381746	Polygon	Vegetations	WS-2	C	85	44.82353	8.964706
383132	Polygon	Barren Land	WS-2	C	86	41.34884	8.269768
384209	Polygon	Water	WS-2	C	100	0	0
263	Polygon	Snow/Ice	WS-3	C	98	5.183673	1.036735
264	Polygon	Barren Land	WS-3	C	86	41.34884	8.269768
269	Polygon	Vegetations	WS-3	C	85	44.82353	8.964706
1264	Polygon	Barren Land	WS-4	D	89	31.39326	6.278652
1837	Polygon	Snow/Ice	WS-4	D	98	5.183673	1.036735
2555	Polygon	Vegetations	WS-4	D	88	34.63636	6.927272

| 2084 | Polygon | Snow/Ice | WS-4 | C | 98 | 5.183673 | 1.036735 |
2158	Polygon	Barren Land	WS-4	C	86	41.34884	8.269768
2567	Polygon	Vegetations	WS-4	C	85	44.82353	8.964706
127942	Polygon	Snow/Ice	WS-5	C	98	5.183673	1.036735
129938	Polygon	Vegetations	WS-5	C	85	44.82353	8.964706
130065	Polygon	Built-up	WS-5	C	91	5.183673	1.036735
130422	Polygon	Trees	WS-5	C	77	75.87013	15.17403
131274	Polygon	Water	WS-5	C	100	0	0
156846	Polygon	Barren Land	WS-6	C	86	41.34884	8.269768
157475	Polygon	Trees	WS-6	C	77	75.87013	15.17403
157571	Polygon	Vegetations	WS-6	C	85	44.82353	8.964706
160555	Polygon	Snow/Ice	WS-6	C	98	5.183673	1.036735
173402	Polygon	Water	WS-6	C	100	0	0
167119	Polygon	Crops	WS-6	C	74	89.24324	17.84865
175467	Polygon	Trees	WS-6	D	85	44.82353	8.964706
175806	Polygon	Vegetations	WS-6	D	88	34.63636	6.927272
176128	Polygon	Snow/Ice	WS-6	D	98	5.183673	1.036735
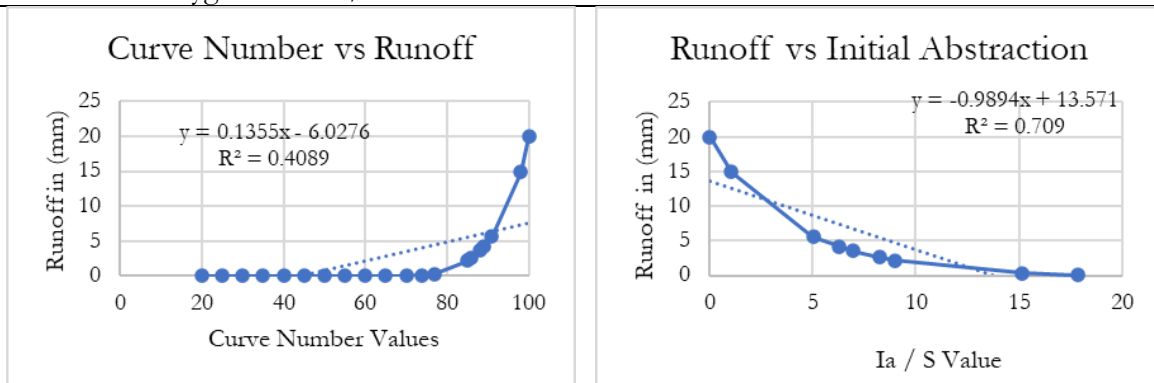
Figure 14: Runoff vs Curve Number and Runoff vs Initial Abstriction

Conclusion and Recommendations:

The application of Geographic Information Systems (GIS) in hydrologic modeling and water resource management is crucial for effectively analyzing and managing large datasets associated with water resources. However, the processing of such large datasets requires significant computing resources, which can be challenging for traditional computing environments. To address this challenge, the developed runoff model leverages the powerful computing environment of Google Earth Engine. Google Earth Engine provides a scalable platform for processing big data in minutes [46], overcoming the limitations of traditional computing resources and saving valuable time in the modeling process. In the runoff model, various data inputs are incorporated, including soil data, land cover data, rainfall data, and Antecedent Moisture Conditions (AMC However, it is important to remember that the model's default Curve Number (CN) for water bodies and snow may not always accurately reflect their hydrological characteristics. A CN of 98-100 may be good for water bodies, however it is not appropriate for snow-covered terrain.

To increase the model's accuracy, recommendations include improving the CN values assigned to snow-covered locations. This can be done by taking into account additional variables such as temperature, which are critical in determining snowmelt processes. Incorporating temperature data enables the computation of growing degree days or melting degree days, which can then be used to obtain more accurate CN values for snow-covered terrain. By fine-tuning the CN values based on temperature data, the runoff model may deliver more realistic

simulations of hydrological processes in snow-covered locations, thereby enhancing hydrologic modelling and water resource management efficiency.

References:

[1]   W. Shi and N. Wang, "An Improved SCS-CN Method Incorporating Slope, Soil Moisture, and Storm Duration Factors for Runoff Prediction," Water 2020, Vol. 12, Page 1335, vol. 12, no. 5, p. 1335, May 2020, doi: 10.3390/W12051335.

[2]   N. Gedney, P. M. Cox, R. A. Betts, O. Boucher, C. Huntingford, and P. A. Stott, "Detection of a direct carbon dioxide effect in continental river runoff records," Nat. 2006 4397078, vol. 439, no. 7078, pp. 835–838, Feb. 2006, doi: 10.1038/nature04504.

[3]   H. Chu, J. Wei, J. Qiu, Q. Li, and G. Wang, "Identification of the impact of climate change and human activities on rainfall-runoff relationship variation in the Three-River Headwaters region," Ecol. Indic., vol. 106, p. 105516, Nov. 2019, doi: 10.1016/J.ECOLIND.2019.105516.

[4]   Y. Xu, S. Wang, X. Bai, D. Shu, and Y. Tian, "Runoff response to climate change and human activities in a typical karst watershed, SW China," PLoS One, vol. 13, no. 3, p. e0193073, Mar. 2018, doi: 10.1371/JOURNAL.PONE.0193073.

[5]   N. Akhtar, M. I. Syakir Ishak, S. A. Bhawani, and K. Umar, "Various Natural and Anthropogenic Factors Responsible for Water Quality Degradation: A Review," Water 2021, Vol. 13, Page 2660, vol. 13, no. 19, p. 2660, Sep. 2021, doi: 10.3390/W13192660.

[6]   S. K. Mishra and V. P. Singh, "Validity and extension of the SCS-CN method for computing infiltration and rainfall-excess rates," Hydrol. Process., vol. 18, no. 17, pp. 3323–3345, Dec. 2004, doi: 10.1002/HYP.1223.

[7]   M. Lal et al., "Evaluation de la méthode du numéro de courbe du Service de la Conservation des Sols à partir de données provenant de parcelles agricoles," Hydrogeol. J., vol. 25, no. 1, pp. 151–167, Feb. 2017, doi: 10.1007/S10040-016-1460-5/METRICS.

[8]   S. Verma, R. K. Verma, S. K. Mishra, A. Singh, and G. K. Jayaraj, "A revisit of NRCS-CN inspired models coupled with RS and GIS for runoff estimation," Hydrol. Sci. J., vol. 62, no. 12, pp. 1891–1930, Sep. 2017, doi: 10.1080/02626667.2017.1334166.

[9]   L. H. Sujud and H. H. Jaafar, "A global dynamic runoff application and dataset based on the assimilation of GPM, SMAP, and GCN250 curve number datasets," Sci. Data 2022 91, vol. 9, no. 1, pp. 1–11, Nov. 2022, doi: 10.1038/s41597-022-01834-0.

[10]   A. W. Dhawale, "Runoff Estimation for Darewadi Watershed using RS and GIS 47", [Online]. Available: https://www.ijrte.org/wp-content/uploads/papers/v1i6/F0413021613.pdf

[11]   "Estimation of Runoff by using SCS Curve Number Method and Arc GIS." Accessed: Jun. 16, 2024. [Online]. Available: https://www.researchgate.net/publication/290947015_Estimation_of_Runoff_by_using_SCS_Curve_Number_Method_and_Arc_GIS

[12]   W. Shi and N. Wang, "Improved SMA-based SCS-CN method incorporating storm duration for runoff prediction on the Loess Plateau, China," Hydrol. Res., vol. 51, no. 3, pp. 443–455, Jun. 2020, doi: 10.2166/NH.2020.140.

[13]   P. K. Singh, S. K. Mishra, R. Berndtsson, M. K. Jain, and R. P. Pandey, "Development of a Modified SMA Based MSCS-CN Model for Runoff Estimation," Water Resour. Manag., vol. 29, no. 11, pp. 4111–4127, Sep. 2015, doi: 10.1007/S11269-015-1048-1/METRICS.

[14]   H. Haider et al., "Appraisal of Climate Change and Its Impact on Water Resources of Pakistan: A Case Study of Mangla Watershed," Atmos. 2020, Vol. 11, Page 1071, vol. 11, no. 10, p. 1071, Oct. 2020, doi: 10.3390/ATMOS11101071.

[15]   U. W. Humphries et al., "Runoff Estimation Using Advanced Soft Computing Techniques: A Case Study of Mangla Watershed Pakistan," Water 2022, Vol. 14, Page 3286, vol. 14, no. 20, p. 3286, Oct. 2022, doi: 10.3390/W14203286.

[16]   M. Yaseen, G. Nabi, M. Latif, and C. Author, "Assessment of Climate Change at Spatio-Temporal Scales and its Impact on Stream Flows in Mangla Watershed," Pakistan J. Eng.

Appl. Sci., vol. 15, pp. 17–36, 2014, Accessed: Jun. 16, 2024. [Online]. Available: https://journal.uet.edu.pk/ojs_old/index.php/pjeas/article/view/91

[17] M. J. Butt, R. Mahmood, and A. Waqas, "Sediments deposition due to soil erosion in the watershed region of Mangla Dam," Environ. Monit. Assess., vol. 181, no. 1–4, pp. 419–429, Oct. 2011, doi: 10.1007/S10661-010-1838-0/METRICS.

[18] M. Azmat, F. Laio, and D. Poggi, "Estimation of water resources availability and mini-hydro productivity in high-altitude scarcely-gauged watershed," Water Resour. Manag., vol. 29, no. 14, pp. 5037–5054, Nov. 2015, doi: 10.1007/S11269-015-1102-Z/METRICS.

[19] K. M. Kent, "NATIONAL ENGINEERING HANDBOOK SECTION 4 HYDROLOGY CHAPTER 15. TRAVEL TIME, TIME OF CONCENTRATION. AND LAG".

[20] H. Mckeever, V., Owen, W., Rallison, R., Engineers, "NATIONAL ENGINEERING HANDBOOK SECTION 4".

[21] H. Sutradhar and W.-C. Liu, "Surface Runoff Estimation Using SCS-CN Method in Siddheswari River Basin, Eastern India," J. Geogr. Environ. Earth Sci. Int., vol. 17, no. 2, pp. 1–9, Sep. 2018, doi: 10.9734/JGEESI/2018/44076.

[22] S. Satheeshkumar, S. Venkateswaran, and R. Kannan, "Rainfall–runoff estimation using SCS–CN and GIS approach in the Pappiredipatti watershed of the Vaniyar sub basin, South India," Model. Earth Syst. Environ. 2017 31, vol. 3, no. 1, pp. 1–8, Feb. 2017, doi: 10.1007/S40808-017-0301-4.

[23] N. N. . Vannasy M., "Estimating Direct Runoff from Storm Rainfall Using NRCS Runoff Method and GIS Mapping in Vientiane City, Laos", [Online]. Available: http://article.nadiapub.com/IJGDC/vol9_no4/23.pdf

[24] C. Strapazan, I. A. Irimuș, G. Șerban, T. C. Man, and L. Sassebes, "Determination of Runoff Curve Numbers for the Growing Season Based on the Rainfall–Runoff Relationship from Small Watersheds in the Middle Mountainous Area of Romania," Water 2023, Vol. 15, Page 1452, vol. 15, no. 8, p. 1452, Apr. 2023, doi: 10.3390/W15081452.

[25] S. K. Mishra, M. K. Jain, P. Suresh Babu, K. Venugopal, and S. Kaliappan, "Comparison of AMC-dependent CN-conversion formulae," Water Resour. Manag., vol. 22, no. 10, pp. 1409–1420, Jan. 2008, doi: 10.1007/S11269-007-9233-5/METRICS.

[26] S. K. Mishra, R. P. Pandey, M. K. Jain, and V. P. Singh, "A rain duration and modified AMC-dependent SCS-CN procedure for long duration rainfall-runoff events," Water Resour. Manag., vol. 22, no. 7, pp. 861–876, Jul. 2008, doi: 10.1007/S11269-007-9196-6/METRICS.

[27] R. Amutha and P. Porchelvan, "Estimation of surface runoff in malattar sub-watershed using SCS-cn method," J. Indian Soc. Remote Sens., vol. 37, no. 2, pp. 291–304, Oct. 2009, doi: 10.1007/S12524-009-0017-7/METRICS.

[28] H. Blanco-Canqui and R. Lal, "Soil Resilience and Conservation," Princ. Soil Conserv. Manag., pp. 425–447, 2010, doi: 10.1007/978-1-4020-8709-7_16.

[29] E. Walker and V. Venturini, "Land surface evapotranspiration estimation combining soil texture information and global reanalysis datasets in Google Earth Engine," Remote Sens. Lett., vol. 10, no. 10, pp. 929–938, Oct. 2019, doi: 10.1080/2150704X.2019.1633487.

[30] M. Shahid et al., "Assessing the potential and hydrological usefulness of the CHIRPS precipitation dataset over a complex topography in Pakistan," Hydrol. Sci. J., vol. 66, no. 11, pp. 1664–1684, Aug. 2021, doi: 10.1080/02626667.2021.1957476.

[31] F. J. Tapiador et al., "Global precipitation measurement: Methods, datasets and applications," Atmos. Res., vol. 104–105, pp. 70–97, Feb. 2012, doi: 10.1016/J.ATMOSRES.2011.10.021.

[32] G. J. Huffman et al., "Integrated Multi-satellite Retrievals for the Global Precipitation Measurement (GPM) Mission (IMERG)," Adv. Glob. Chang. Res., vol. 67, pp. 343–353, 2020, doi: 10.1007/978-3-030-24568-9_19.

[33] C. Kummerow et al., "The Status of the Tropical Rainfall Measuring Mission (TRMM) after Two Years in Orbit," J. Appl. Meteorol. Climatol., vol. 39, no. 12, pp. 1965–1982, Dec.

2000, doi: 10.1175/1520-0450(2001)040.

[34] R. Jain, S., Jaiswal, R. K., Lohani, A. K., Galkate, "Development of cloud-based rainfall-run-off model using Google Earth Engine," 2021, [Online]. Available: https://www.currentscience.ac.in/Volumes/121/11/1433.pdf

[35] Z. Shen et al., "Recent global performance of the Climate Hazards group Infrared Precipitation (CHIRP) with Stations (CHIRPS)," J. Hydrol., vol. 591, p. 125284, Dec. 2020, doi: 10.1016/J.JHYDROL.2020.125284.

[36] J. S. Theon, "The tropical rainfall measuring mission (TRMM)," Adv. Sp. Res., vol. 14, no. 3, pp. 159–165, Mar. 1994, doi: 10.1016/0273-1177(94)90210-0.

[37] M. Babur, M. S. Babel, S. Shrestha, A. Kawasaki, and N. K. Tripathi, "Assessment of Climate Change Impact on Reservoir Inflows Using Multi Climate-Models under RCPs—The Case of Mangla Dam in Pakistan," Water 2016, Vol. 8, Page 389, vol. 8, no. 9, p. 389, Sep. 2016, doi: 10.3390/W8090389.

[38] Y. T. Dile and R. Srinivasan, "Evaluation of CFSR climate data for hydrologic prediction in data-scarce watersheds: an application in the Blue Nile River Basin," JAWRA J. Am. Water Resour. Assoc., vol. 50, no. 5, pp. 1226–1241, Oct. 2014, doi: 10.1111/JAWR.12182.

[39] D. R. Fuka, M. T. Walter, C. Macalister, A. T. Degaetano, T. S. Steenhuis, and Z. M. Easton, "Using the Climate Forecast System Reanalysis as weather input data for watershed models," Hydrol. Process., vol. 28, no. 22, pp. 5613–5623, Oct. 2014, doi: 10.1002/HYP.10073.

[40] S. J. Bhuyan, K. R. Mankin, and J. K. Koelliker, "WATERSHED–SCALE AMC SELECTION FOR HYDROLOGIC MODELING," Trans. ASAE, vol. 46, no. 2, pp. 303-, Mar. 2003, doi: 10.13031/2013.12981.

[41] N. Y. Krakauer, T. Lakhankar, and G. H. Dars, "Precipitation Trends over the Indus Basin," Clim. 2019, Vol. 7, Page 116, vol. 7, no. 10, p. 116, Sep. 2019, doi: 10.3390/CLI7100116.

[42] A. P. Dimri et al., "Western Disturbances: A review," Rev. Geophys., vol. 53, no. 2, pp. 225–246, 2015, doi: 10.1002/2014RG000460.

[43] M. S. Hussain and S. Lee, "Investigation of summer monsoon rainfall variability in Pakistan," Meteorol. Atmos. Phys., vol. 128, no. 4, pp. 465–475, Aug. 2016, doi: 10.1007/S00703-015-0423-Z/METRICS.

[44] M. Adnan et al., "Variability and Predictability of Summer Monsoon Rainfall over Pakistan," Asia-Pacific J. Atmos. Sci., vol. 57, no. 1, pp. 89–97, Feb. 2021, doi: 10.1007/S13143-020-00178-2/METRICS.

[45] H. M. B. Wang, Y., "Application of the SCSCN method on runoff estimation in small watershed on Loess Plateau," Sci. Soil Water Conserv., vol. 6, no. 6, pp. 87–91, 2008.

[46] H. Tamiminia, B. Salehi, M. Mahdianpari, L. Quackenbush, S. Adeli, and B. Brisco, "Google Earth Engine for geo-big data applications: A meta-analysis and systematic review," ISPRS J. Photogramm. Remote Sens., vol. 164, pp. 152–170, Jun. 2020, doi: 10.1016/J.ISPRSJPRS.2020.04.001.